Journal of Nuclear Medicine, published on June 30, 2022 as doi:10.2967/jnumed.122.264126

Improved tumor responses with sequential targeted alpha followed by IL2 immunocytokine therapies in treatment of CEA positive breast and colon tumors in CEA transgenic mice

Megan Minnix[1*], Maciej Kujawski[1*], Erasmus Poku[2], Paul J. Yazaki[1], Jeffrey Y. Wong[3] and John E. Shively[1#]

[1] Department of Immunology and Theranostics, Riggs Institute of Diabetes and Metabolic Research, Beckman Research Institute of the City of Hope, Duarte, CA 91010.

[2] Radiopharmacy, Beckman Research Institute of the City of Hope, Duarte, CA 91010.

[3] Department of Radiation Oncology, City of Hope National Medical Center, Duarte, CA 91010.

[*] These authors contributed equally to this research.

[#] To whom to address correspondence: John Shively, Department of Immunology and Theranostics, 1500 East Duarte Rd. Duarte, CA 91010, jshively@coh.org.

Running title: Targeted α and immunocytokine therapy

Authors Disclosures**:** The authors declare no conflict of interest.

Word count: 5144.

ABSTRACT

Rationale: Targeted alpha therapy (TAT) delivers high linear transfer energy alpha particles to tumors with the potential to generate tumor immune responses that may be augmented by antigen targeted immunotherapy. Methods: This concept was evaluated in immunocompetent carcinoembryonic antigen (CEA) transgenic mice bearing CEA positive mammary or colon tumors. Tumors were targeted with humanized anti-CEA antibody M5A labeled with ^{225}Ac for its 10-day half-life and emission of 4 alpha particles, and the immunocytokine M5A-IL2. Results: A dose response (3.7, 7.4 and 11.1 kBq) of TAT only, for orthotopic CEA positive mammary tumors, was observed with a tumor growth delay of 30d and an increase in median survival from 20d to 36d at the highest dose. ICK (4x daily) monotherapy gave a tumor growth delay of 20d that was not improved by addition of 7.4 kBq of TAT 5d after the start of immunocytokine. However, TAT (7.4 kBq) followed by ICK 10d later led to a tumor growth delay of 38d with an increase of median survival to 45d. Similar results were seen for TAT followed by immunocytokine at 5d vs 10d. When a similar study was performed with subcutaneous implanted CEA positive MC38 colon tumors, TAT (7.4 kBq) monotherapy gave an increase in median survival from 29d to 42d. The addition of ICK 10d post 7.4 kBq TAT increased median survival to 57d. Immunophenotyping showed increased tumor infiltrating IFNγ^+CD8$^+$ T-cells and an increased ratio of these cells to Foxp3$^+$CD4$^+$ Tregs with sequential therapy. Immunohistochemistry confirmed there was an increase in tumor-infiltrating CD8$^+$ T-cells in the sequential therapy group, strongly suggesting that ICK augmented TAT can lead to an immune response that improves tumor therapy. Conclusion: Low dose (7.4 kBq) TAT followed by a 4 dose immunocytokine regimen 5 or 10 days later gave superior tumor reductions and survival curves compared to either monotherapy in breast and colon cancer tumor models. Reversing the order of therapy to immunocytokine followed by TAT 10 days later was equivalent to either monotherapy in the breast cancer model.

INTRODUCTION

Carcinoembryonic antigen (CEA, CEACAM5) is a pancarcinoma antigen highly expressed in colon (*1*) and breast cancers. Radiolabeled CEA antibodies have been used to image a variety of CEA expressing tumors (*2-4*), confirming their tumor targeting specificity. Since most anti-CEA antibodies are not cytotoxic, they require the conjugation to drugs or radionuclides for therapeutic applications. In this respect radioimmunotherapy with anti-CEA antibodies radiolabeled with the beta-emitters ^{131}I (*5-7*) or ^{90}Y (*8,9*) have met with some success in the clinic. In the case of immunotherapy, anti-CEA bifunctional antibodies have shown promising preclinical results (*10,11*). In addition, there are also several clinical trials (NCT04513431, NCT04348643, NCT02349724) investigating CAR T cell therapy targeting CEA, that have met with mixed results (*12*). Thus, there is an unmet need for improvement in CEA targeted therapies.

Sequential targeted radiotherapy followed by targeted immunotherapy is a promising approach in that it may stimulate an immune response. In this respect, we have recently shown that stereotactic body radiotherapy plus a CEA targeted immunocytokine gave superior tumor reduction than either monotherapy (*13*). Those studies were performed with humanized anti-CEA antibody M5A (*14*) and an M5A-IL2 fusion protein (*13*). We now extend those studies to sequential targeted alpha-therapy (TAT) plus immunocytokine. The choice of alpha- over beta- based radionuclide therapy is based on the fact that alpha-emitters deliver more energy to the tumor and tumor vasculature due to their high linear energy transfer (*15*) with a potential increase in tumor cytotoxicity due to stimulation of an immune response. In addition, their low tissue penetration is expected to reduce the hematologic toxicity of the systemic radiolabeled antibody, one of the major off-target effects of beta-emitter based RIT (*16*). For this study, we chose the alpha-emitter ^{225}Ac for its long half-life (10 days) and emission of four alpha-particles (*17*). We have previously investigated the use of ^{225}Ac-based TAT in the treatment of ovarian cancer (*18*) and multiple myeloma (*19*), finding that in one study, ^{225}Ac-radionuclide TAT was superior to ^{177}Lu-radionuclide RIT (*19*).

We hypothesized that TAT was more likely to stimulate a tumor immune response when followed with targeted immunotherapy. In order to test this hypothesis, it was necessary to perform these studies in immune competent mice that expressed the target antigen of interest in normal tissues. For this reason, we utilized CEA transgenic mice in which the entire human CEA gene was expressed, conferring tissue specific CEA expression that mimics that found in

man (*20*). We have previously shown that an all murine anti-CEA immunocytokine significantly reduced CEA positive tumor growth in this CEA transgenic model (*21*), and more recently, that an all murine anti-CEA CAR T plus the humanized immunocytokine reduced tumor growth in the same model (*22*). We now show that sequential TAT followed by immunocytokine therapy significantly improves tumor responses in both breast and colon tumors compared to either monotherapy in the CEA transgenic model.

Materials

M5A, DOTA-M5A, immunocytokine, and the cell lines E0771/CEA and MC38/CEA were previously described (*13*).

Radiolabeling

DOTA-M5A (50 μg) was incubated with ^{225}Ac at a labeling ratio of 1.85 kBq/μg for 45 min at 43°C, chased with 1 mM DTPA and purified by SE-HPLC.

Immunohistochemistry, blood analysis and flow cytometry

Details of immunohistochemistry staining blood analysis and flow cytometry are provided in Supplemental Data.

Animal Studies

Animal handling was done in accordance with IACUC protocol 91017 approved by the City of Hope Institutional Animal Care and Use Committee. CEA transgenic mice were previously described (*20*). E0771/CEA cells (1E5 in Matrigel:PBS 1:1) were injected into the mammary fat pad, and MC38/CEA (1E6) subcutaneously.

Statistical Analysis

Two-way ANOVA was used to analyze tumor growth curves and log-rank Mantel-Cox for survival curves using Prism 8.3.0 (GraphPad Software). Survival was time in which the tumor reached 1500 mm^3. Treated groups were compared to untreated, unless otherwise stated. Differences were considered significant if $P \leq 0.05$.

RESULTS

Targeted alpha therapy of E0771/CEA mammary tumors

Murine mammary cancer cells E0771 transfected with CEA (*13*) were injected into the mammary fat pad of CEA transgenic mice (*20*) to establish mammary tumors in a immunocompetent model that expressed the human CEA gene. Since we have previously shown that these tumors do not respond to naked humanized anti-CEA antibody M5A (*13*), we tested their response to TAT using ^{225}Ac-DOTA-M5A (Fig. 1A**)**. Increasing doses from 3.7 kBq to 11.1 kBq showed a significant dose response compared to untreated controls (Fig. 1B and Supplemental Table 1) with the highest dose leading to a delay in tumor growth of about 30d and a significant increase in median survival from ~20d to 36d compared to untreated controls (Fig. 1C and Supplemental Table 1). Whole body toxicity as measured by weight loss (≥20% loss) was not observed at all doses (Fig. 1D). In addition, there was no evidence of acute liver or kidney toxicity as measured by enzymes at the end of the study (Supplemental Table 2).

Flow cytometry analysis of the blood at d21 indicated a significant decrease of CD8 T-cells and B cells for the two highest doses of TAT with no effect on CD11b myeloid cells (Supplemental Fig. 1A). The highest dose of TAT significantly reduced tumor infiltration of both CD4 and CD8 T-cells (Supplemental Fig. 1B) and an increase of tumor infiltrating neutrophils by 7.4 kBq and 11.1 kBq TAT (Supplemental Fig. 1C). These results suggest the possibility that TAT had a major effect on the immune response to the tumor, but it was unclear if the effect was immunosuppressive or immunostimulatory.

Comparison of immunocytokine + TAT vs TAT + immunocytokine in E0771/CEA mammary tumors

The order of sequential therapy was tested since it was likely that TAT could kill tumor resident CD8 cells that would otherwise respond to immunocytokine given first (Fig. 2A). The immunocytokine therapy schedule of 4 daily doses of 1 mg/kg starting at 8d after tumor inoculation into the mammary fat pad adopted from our previous study (*13*), gave a significant delay of tumor growth of about 20d compared to untreated tumors (orange curve, Fig. 2B; Supplemental Table 1). Interestingly, the delay in tumor growth for immunocytokine therapy alone was equivalent to the 7.4 kBq of TAT only (green curve**,** Fig. 2B). When immunocytokine K was given prior to TAT (pink curve Fig. 2B), the results were similar to either monotherapy. Thus, the addition of TAT to immunocytokine given first therapy provided no boost to the anti-tumor response.

For TAT first followed by immunocytokine, we chose 10d later for the start of immunocytokine, based on the 2-4 day half-life of the circulating antibody in the blood (*23*) and the 10d half-life of ^{225}Ac. When TAT was followed by immunocytokine K 10d later, tumor growth was reduced to 38d (purple curve, Fig. 2B) with an increase in median survival to 45d compared to either monotherapy of ~30d (Fig. 2C**,** Supplemental Tables 1 and 3). In addition, sequential therapy did not result in significant loss of whole body weight (Supplemental Fig. 2A) or liver and kidney toxicity (Supplemental Table 2). White blood cell (WBC) analysis of TAT followed by immunocytokine showed a 50% reduction early after therapy (21d) that recovered at the late time point (30-50d) (Supplemental Fig. 2B). A breakdown of WBC into component cells revealed early effects in this group were mostly on lymphocytes and neutrophils with recovery in the TAT + immunocytokine group by the later time point (Supplemental Fig. 2C-D**).** There was no effect on red blood cells (RBC) in any group (Supplemental Fig. 2E**)** and about a 50% reduction in platelets immediately following therapy that recovered at the end of the study **(**Supplemental Fig. 2F**).** Overall, the toxicities of the sequential therapies were transient and minimal.

TAT alone or TAT + immunocytokine affected the cellular viability of treated tumors at 21d as shown by flow cytometry (Supplemental Fig. 3A). Although the percentage of tumor infiltrating CD8 or CD4 T-cells were reduced by TAT only and increased by immunocytokine monotherapy, the changes were not statistically significant. However, when analyzed for IFNγ production, there was a significant increase of tumor infiltrating IFNγ^+ CD8$^+$ T-cells at 21d (Supplemental Fig. 3B) of which IFNγ^+PD-1$^+$ tumor infiltrating CD8$^+$ T-cells also increased, followed by a significant decrease of IFNγ^-PD-1$^+$ exhausted T cells (Supplemental Fig. 3C). In addition, the ratio of CD8$^+$IFNγ^+ to CD4$^+$Treg cells increased in both the immunocytokine only and sequential therapy groups (Supplemental Fig. 3D), suggesting that the Tregs play a more important role in the tumor response than the percentage of PD1$^+$ CD8$^+$ T-cells. This analysis confirmed that TAT followed by immunocytokine was superior to immunocytokine followed by TAT, suggesting that TAT adversely affected immunocytokine given first in sequential therapy.

Timing of immunocytokine after TAT in E0771/CEA mammary tumors

Since TAT can adversely affect immunocytokine therapy when immunocytokine is given first but not when immunocytokine was given 10d after TAT, we tested the possibility of administrating immunocytokine 5d post TAT (Fig. 3A**)**. Five days was chosen as a time point when circulating M5A is at about 25% of initial levels (*24*) and total ^{225}Ac would be at about 50%

of its initial levels. Although the tumor reduction and survival curves showed slight differences between immunocytokine 5d vs 10d after TAT, overall, the results were statistically identical vs untreated controls and monotherapies (Fig. 3B-C, Supplemental Table 1). A comparison of median survivals for all the mammary tumor studies shows increased survivals for the +5d and +10d groups out to 44-45d (Supplemental Table 3**)**. Flow analysis of infiltrating leukocytes in the tumor were also similar between the two sequential therapy groups (Supplemental Fig. 4A-C). Notably, the percent $CD4^+$ $Foxp3^+$ Tregs was reduced (Supplemental Fig. 4C**)**-and $IFN\gamma^+CD8^+$ cells to Tregs ratio was higher in the +10d and +5d immunocytokine groups (Supplemental Fig. 4D). We conclude that delaying immunocytokine after TAT may prove to be beneficial as early as 5d post TAT. This result suggests that immunocytokine may have its greatest effects on tumors that are damaged by prior radiation therapy, whether SBRT or TAT.

There was a minimal effect of timing of immunocytokine post TAT on whole body toxicity (Supplemental Fig. 5) or liver and kidney toxicity (Supplemental Table 2). Hematological analysis was similar between the two studies showing reduction of lymphocytes with TAT only at the early time point, and recovery in the TAT + immunocytokine group at the late time point (Supplemental Fig. 5A-D). There were no effects on RBC (Supplemental Fig. 5E) and a transient effect on platelets (Supplemental Fig. 5F).

TAT of CEA positive MC38/CEA colon tumors

To confirm the efficacy of TAT in a second tumor model, CEA transfected murine colon carcinoma MC38 cells were engrafted s.c. in CEA transgenic mice. In a dose response study of 3.7- 11.1 kBq, there was little difference in tumor reduction or survival between control and treated tumors at the lowest dose (blue vs orange curves Fig. 4A-B, Supplemental Table 1), but at the middle (7.4 kBq) and highest (11.1 kBq) dose, there was a significant reduction in tumor growth and increase in median survival from 29 days (no treatment) to 50 days for the highest dose (Supplemental Table 4). In the colon cancer model we evaluated the effects of increased TAT by changing the dose in two ways, first by raising the maximum dose to 14.8 kBq, and second, by administering the 7.4 kBq dose twice, once at 13d post tumor inoculation and again 10d later. The tumor growth curves for individual mice shown in Fig. 4C reveal an interesting spread in response to TAT, suggesting that minor differences in tumor sizes or microenvironment affect the response to TAT that are not apparent in the control tumors. However, both the tumor growth (Fig. 4C, Supplemental Table 1) and survival curves (Fig. 4D, Supplemental Tables 1 and 4) demonstrate that the single 14.8 kBq dose was superior to the

fractionated 2x 7.4 kBq dose. No significant whole body (Supplemental Figure 6A), liver or kidney (Supplemental Table 5) or chronic hematological (Supplemental Figure 6B-F**)** toxicities were noted in this TAT monotherapy model.

Sequential TAT plus immunocytokine therapy of MC38/CEA colon tumors

In order to directly compare the two tumor model responses to sequential therapy, the identical TAT dose of 7.4 kBq was chosen with a delay of 10d for the start of immunocytokine (Fig. 5A). The tumor growth curves for TAT or immunocytokine monotherapy were identical until 35d after which immunocytokine monotherapy showed tumor regrowth (pink vs green curves, Fig. 5B, Supplemental Table 1). Even though some of the mice treated with TAT had prolonged tumor growth inhibition and survival, the sequential therapy showed an improved tumor growth reduction out to about 45d after which tumor regrowth became obvious (orange curve, Fig. 5B, Supplemental Table 1). Median survival for sequential therapy was 57d vs 29d for untreated controls (Fig. 5C, Supplemental Tables 1 and 4). No whole body (Supplemental Fig. 7A), liver or kidney (Supplemental Table 5) toxicities were noted in the TAT + immunocytokine group; however, early lymphocyte and platelet numbers and percentages were reduced that recovered at the late time point (Supplemental Fig. 7B-F).

Surprisingly, there was a significant increase of tumor infiltrating $CD4^+$ and $CD8^+$ T-cells only in mice treated with immunocytokine as analyzed by flow cytometry at 27d (Supplemental Fig. 8A). However, both $IFN\gamma^+$ $CD4^+$ and $CD8^+$ T-cells were significantly increased by sequential therapy (Supplemental Fig. 8B**).** Since these findings did not explain the significant improvement in tumor growth inhibition and survival in the TAT + immunocytokine group, an additional study was performed in which tumors were collected and analyzed at days 1, 5 and 8 after the last dose of immunocytokine in the sequential therapy group. The results of this study showed a gradual increase of $CD8^+$ T-cells infiltration into tumors (Supplemental Fig. 8C). The increase of tumor infiltrating $IFN\gamma^+$ $CD8^+$ T-cells at days 5 and 8 after the last dose of immunocytokine in sequential therapy group, was especially evident (Supplemental Fig. 8D). As in the other sequential therapy model, the change in the ratio of $IFN\gamma^+$ $CD8^+$ T-cells to regulatory T-cells at day 5 and 8 after last dose of immunocytokine in the sequential therapy group was significant (Supplemental Fig. 8E).

We conclude that both tumor models show a similar augmented response of TAT followed by immunocytokine in which the increase in cytotoxic infiltrating T-cells and decrease in

tumor Tregs are due to the addition of immunocytokine, suggesting an immunological mechanism.

Immunohistochemistry analysis of therapies

A limited number of tumors were harvested 21 or 27 days (for breast or colon cancer models, respectively) after tumor injection to study tumor morphology, vascularity, CEA expression, and lymphocyte infiltration. In the orthotopic mammary tumor model, vascularity as measured by CD31 staining was most affected by sequential therapy as evidenced by increased staining and vessel size especially at the tumor periphery (Supplemental Fig. 9A-D). In the colon cancer model, the vascularity of untreated tumors showed even CD31 staining across the entire tumor that was greatly disrupted in all therapy groups (Supplemental Fig. 9E-H).

CD8 numbers were lowest in the TAT alone breast cancer group, with similar expression in the untreated control and immunocytokine groups and were highest in the TAT+ immunocytokine group (Supplemental Fig. 10A-D). CEA expression was largely limited to the tumor periphery in untreated controls and was markedly decreased towards the tumor center (Supplemental Fig. 10E), indicating in vivo effect on CEA expression in this tumor model. Interestingly, TAT only greatly reduced CEA expression at the tumor periphery while preserving expression towards the tumor center (Supplemental Fig. 10F), while the opposite was true for immunocytokine only therapy (Supplemental Fig. 10G). CEA expression in the sequential therapy tumors was similar to TAT only (Supplemental Fig. 10H), suggesting that TAT was most efficient in killing CEA positive cells at the tumor periphery, a result that may be explained by the low tissue penetration of alpha particles. In addition, breast tumors were stained for macrophages with the antibody F4/80 (Supplemental Fig. 11). In this series, F4-80 staining was most intense at the tumor periphery and relatively unchanged for immunocytokine only therapy. However, TAT alone or TAT + immunocytokine greatly increased myeloid staining throughout the tumor, suggesting that TAT mobilized myeloid infiltration.

For CD8 staining of colon cancer tumors, untreated controls had large numbers of resident CD8 cells (Supplemental Fig. 12A) that were greatly reduced by TAT only (Supplemental Fig. 12B). The profile in immunocytokine only therapy was intermediate with clusters of CD8 cells observed in regions of the tumor (Supplemental Fig. 12C), suggesting a redistribution and/or elimination of CD8 subtypes. Sequential therapy was similar to TAT only

(Supplemental Fig. 12D). CEA staining was uniformly intense throughout the tumor in untreated controls (Supplemental Fig. 12E), but with islands of low staining in TAT only tumors (Supplemental Fig. S8F). Conversely, immunocytokine only treated controls stained lightly for CEA with islands of CEA negative cells (Supplemental Fig. 12G). The sequential therapy tumors showed intense CEA staining at the periphery with a centralized area of less intense staining (Supplemental Fig. 12H). Myeloid cell staining with F4/80 exhibited a profile different from the mammary tumors with intense sporadic staining throughout the untreated controls changing to peripheral tumor staining in the treated groups (Supplemental Fig. 13).

DISCUSSION

Both tumor models responded similarly to targeted monotherapies in which higher doses caused transient WBC and platelet reduction. Although no early kidney toxicity was observed, we did not test for delayed kidney toxicity, a potential problem with ^{225}Ac based therapy (*17*). In the case of the colon cancer model, an even higher dose (14.7 kBq), divided into single or a split treatment regimen, showed that the single higher dose increased the median survival to 65d vs 51d for the split dose.

The order of sequential therapy approaches in the breast cancer model showed immunocytokine first followed by TAT was no better than either monotherapy, but TAT followed by immunocytokine increased survival from 30d to 45d. Since immunocytokine therapy increases CD8 infiltration into both tumor models, these cells may be killed by subsequent TAT that is cytotoxic to all cells in the tumor and T-cells in particular. This may explain the controversial results of tumor targeted radiation therapy that were found to either suppress or stimulate the immune response (*25,26*). Although antibody targeted radiation therapy can deliver significant tumor doses (*27,28*), they are accompanied by hematological doses that are unavoidable due to circulating antibody. However, hematological doses can be reduced by the short range of alpha particles used in TAT (*17*). In a previous study with the same breast cancer model, tumor regrowth with SBRT plus immunocytokine occurred at 23 days vs 15 days with SBRT alone (*13*). Tumor regrowth with TAT plus immunocytokine occurred 40 days vs 20 days for TAT alone. Thus, TAT plus immunocytokine may have advantages compared to SBRT plus immunocytokine. Clinical studies with SBRT plus anti-PD-1 or anti-PD-L1 immunotherapy demonstrate modest improvements in tumor response and suggest that the toxicities associated with these immunotherapies is limiting (*29*). The use of targeted immunotherapy with agents such as immunocytokine may improve outcomes.

IHC staining of tumors showed tumors responded spatially differently for vascular effects, immune cell infiltration and target antigen expression. Notably, TAT was more effective than immunocytokine in destroying or modifying tumor vasculature. CEA expression was most affected by TAT. However, effective therapy was observed in both models, suggesting that loss of CEA expression was not the major factor. Thus, in a single targeted treatment regimen, the initial antigen expression played the dominant role.

Myeloid cell infiltration was pronounced for TAT only or TAT + immunocytokine vs immunocytokine only in both models, but TAT caused little, if any, increase in CD8 cell infiltration, whereas immunocytokine therapy had a greater effect on CD8 infiltration, whether alone or followed by TAT in both models. A role for myeloid cell infiltration after TAT was also noted by Dabagian et al. (*30*) who ascribed this effect as immunosuppressive. Thus, immunotherapy may increase the effectiveness of TAT by reducing myeloid infiltration. In the study by Dabagian et al. (*30*) anti-PD-1 immunotherapy was more effective that TAT, making comparisons to our study difficult.

CONCLUSION

We showed comparable tumor reduction by TAT or immunocytokine monotherapy in two tumor models, that when performed sequentially with TAT followed by immunocytokine produced improved therapy. Both mono and sequential therapies have minimal whole body, hematological, liver and kidney toxicities. Increased infiltration of IFNγ^+CD8 lymphocytes and an increased ratio of the IFNγ^+CD8 to FoxP$^+$CD4 T-cells is a mechanistic observation for immunocytokine only or sequential TAT + immunocytokine therapy in both tumor models.

Authors Contributions

MM and MK: data curation, formal analysis and original draft; EP and PJY data curation; JYW and JES: funding acquisition, review and editing.

Acknowledgements

This research was partially supported by NIH cancer center support grant P30CA033572.

KEY POINTS

QUESTION: Is sequential targeted alpha therapy (TAT) plus targeted immunocytokine therapy more effective than either monotherapy, and what is the best order of sequential targeted therapies?

PERTINENT FINDINGS: In an immunocompetent animal model TAT followed by immunocytokine was more effective than either monotherapy, and TAT before immunocytokine performed better than immunocytokine followed by TAT. A major effect of immunocytokine was to improve the effector CD8 T-cell to Treg ratio.

IMPLICATIONS FOR PATIENT CARE: The effect of targeted radiotherapy on the immune system is controversial, making it hard to predict if and when targeted immunotherapy should be added to the treatment regimen. Our study suggests that TAT followed by immunocytokine may be effective due to the limited tissue range of alpha particles that cause less hematological immune suppression.

REFERENCES

1. Tong G, Xu W, Zhang G, et al. The role of tissue and serum carcinoembryonic antigen in stages I to III of colorectal cancer-A retrospective cohort study. *Cancer Med.* 2018;7:5327-5338.

2. Buchegger F, Mach JP, Pelegrin A, et al. Radiolabeled chimeric anti-CEA monoclonal antibody compared with the original mouse monoclonal antibody for surgically treated colorectal carcinoma. *J Nucl Med.* 1995;36:420-429.

3. Goldenberg DM. Cancer imaging with CEA antibodies: historical and current perspectives. *Int J Biol Markers.* 1992;7:183-188.

4. Wong JY, Thomas GE, Yamauchi D, et al. Clinical evaluation of indium-111-labeled chimeric anti-CEA monoclonal antibody. *J Nucl Med.* 1997;38:1951-1959.

5. Behr TM, Sharkey RM, Juweid ME, et al. Phase I/II clinical radioimmunotherapy with an iodine-131-labeled anti-carcinoembryonic antigen murine monoclonal antibody IgG. *J Nucl Med.* 1997;38:858-870.

6. Juweid ME, Sharkey RM, Behr T, et al. Radioimmunotherapy of patients with small-volume tumors using iodine-131-labeled anti-CEA monoclonal antibody NP-4 F(ab')2. *J Nucl Med.* 1996;37:1504-1510.

7. Ychou M, Azria D, Menkarios C, et al. Adjuvant radioimmunotherapy trial with iodine-131-labeled anti-carcinoembryonic antigen monoclonal antibody F6 F(ab')2 after resection of liver metastases from colorectal cancer. *Clin Cancer Res.* 2008;14:3487-3493.

8. Akhavan D, Yazaki P, Yamauchi D, et al. Phase I study of Yttrium-90 radiolabeled M5A anti-carcinoembryonic antigen humanized antibody in patients with advanced carcinoembryonic antigen producing malignancies. *Cancer Biother Radiopharm.* 2020;35:10-15.

9. Wong JY, Chu DZ, Williams LE, et al. A phase I trial of (90)Y-DOTA-anti-CEA chimeric T84.66 (cT84.66) radioimmunotherapy in patients with metastatic CEA-producing malignancies. *Cancer Biother Radiopharm.* 2006;21:88-100.

10. Oberst MD, Fuhrmann S, Mulgrew K, et al. CEA/CD3 bispecific antibody MEDI-565/AMG 211 activation of T cells and subsequent killing of human tumors is independent of mutations commonly found in colorectal adenocarcinomas. *MAbs.* 2014;6:1571-1584.

11. Bacac M, Fauti T, Sam J, et al. A novel carcinoembryonic antigen T-cell bispecific antibody (CEA TCB) for the treatment of solid tumors. *Clin Cancer Res.* 2016;22:3286-3297.

12. Zhang C, Wang Z, Yang Z, et al. Phase I escalating-dose trial of CAR-T therapy targeting CEA(+) metastatic colorectal cancers. *Mol Ther.* 2017;25:1248-1258.

13. Kujawski M, Sherman M, Hui S, et al. Potent immunomodulatory effects of an anti-CEA-IL-2 immunocytokine on tumor therapy and effects of stereotactic radiation. *Oncoimmunology.* 2020;9:1724052.

14. Yazaki PJ, Sherman MA, Shively JE, et al. Humanization of the anti-CEA T84.66 antibody based on crystal structure data. *Protein Engineering, Design and Selection.* 2004;17:481-489.

15. Morgenstern A, Apostolidis C, Kratochwil C, Sathekge M, Krolicki L, Bruchertseifer F. An Overview of targeted alpha therapy with (225)actinium and (213)bismuth. *Curr Radiopharm.* 2018;11:200-208.

16. Ferrer L, Kraeber-Bodere F, Bodet-Milin C, et al. Three methods assessing red marrow dosimetry in lymphoma patients treated with radioimmunotherapy. *Cancer.* 2010;116:1093-1100.

17. Scheinberg DA, McDevitt MR. Actinium-225 in targeted alpha-particle therapeutic applications. *Curr Radiopharm.* 2011;4:306-320.

18. Minnix M, Li L, Yazaki PJ, et al. TAG-72-targeted α-radionuclide therapy of ovarian cancer using (225)Ac-labeled DOTAylated-huCC49 antibody. *J Nucl Med.* 2021;62:55-61.

19. Minnix M, Adhikarla V, Caserta E, et al. Comparison of CD38-targeted α- versus β-radionuclide therapy of disseminated multiple myeloma in an animal model. *J Nucl Med.* 2021;62:795-801.

20. Clarke P, Mann J, Simpson JF, Rickard-Dickson K, Primus FJ. Mice transgenic for human carcinoembryonic antigen as a model for immunotherapy. *Cancer Res.* 1998;58:1469-1477.

21. Xu X, Clarke P, Szalai G, et al. Targeting and therapy of carcinoembryonic antigen-expressing tumors in transgenic mice with an antibody-interleukin 2 fusion protein. *Cancer Res.* 2000;60:4475-4484.

22. Cha SE, Kujawski M, P JY, Brown C, Shively JE. Tumor regression and immunity in combination therapy with anti-CEA chimeric antigen receptor T cells and anti-CEA-IL2 immunocytokine. *Oncoimmunology.* 2021;10:1899469.

23. Li L, Crow D, Turatti F, et al. Site-specific conjugation of monodispersed DOTA-PEGn to a thiolated diabody reveals the effect of increasing peg size on kidney clearance and tumor uptake with improved 64-copper PET imaging. *Bioconjugate chemistry.* 2011;22:709-716.

24. Yazaki PJ, Sherman MA, Shively JE, et al. Humanization of the anti-CEA T84.66 antibody based on crystal structure data. *Protein Eng Des Sel.* 2004;17:481-489.

25. Grass GD, Krishna N, Kim S. The immune mechanisms of abscopal effect in radiation therapy. *Curr Probl Cancer.* 2016;40:10-24.

26. Sridharan V, Schoenfeld JD. Immune effects of targeted radiation therapy for cancer. *Discov Med.* 2015;19:219-228.

27. Muylle K, Flamen P, Vugts DJ, et al. Tumour targeting and radiation dose of radioimmunotherapy with (90)Y-rituximab in CD20+ B-cell lymphoma as predicted by (89)Zr-rituximab immuno-PET: impact of preloading with unlabelled rituximab. *Eur J Nucl Med Mol Imaging.* 2015;42:1304-1314.

28. DeNardo SJ, Williams LE, Leigh BR, Wahl RL. Choosing an optimal radioimmunotherapy dose for clinical response. *Cancer.* 2002;94:1275-1286.

29. Chen Y, Gao M, Huang Z, Yu J, Meng X. SBRT combined with PD-1/PD-L1 inhibitors in NSCLC treatment: a focus on the mechanisms, advances, and future challenges. *J Hematol Oncol.* 2020;13:105.

30. Dabagian H, Taghvaee T, Martorano P, et al. PARP targeted alpha-particle therapy enhances response to PD-1 immune-checkpoint blockade in a syngeneic mouse model of glioblastoma. *ACS Pharmacol Transl Sci.* 2021;4:344-351.

FIGURES

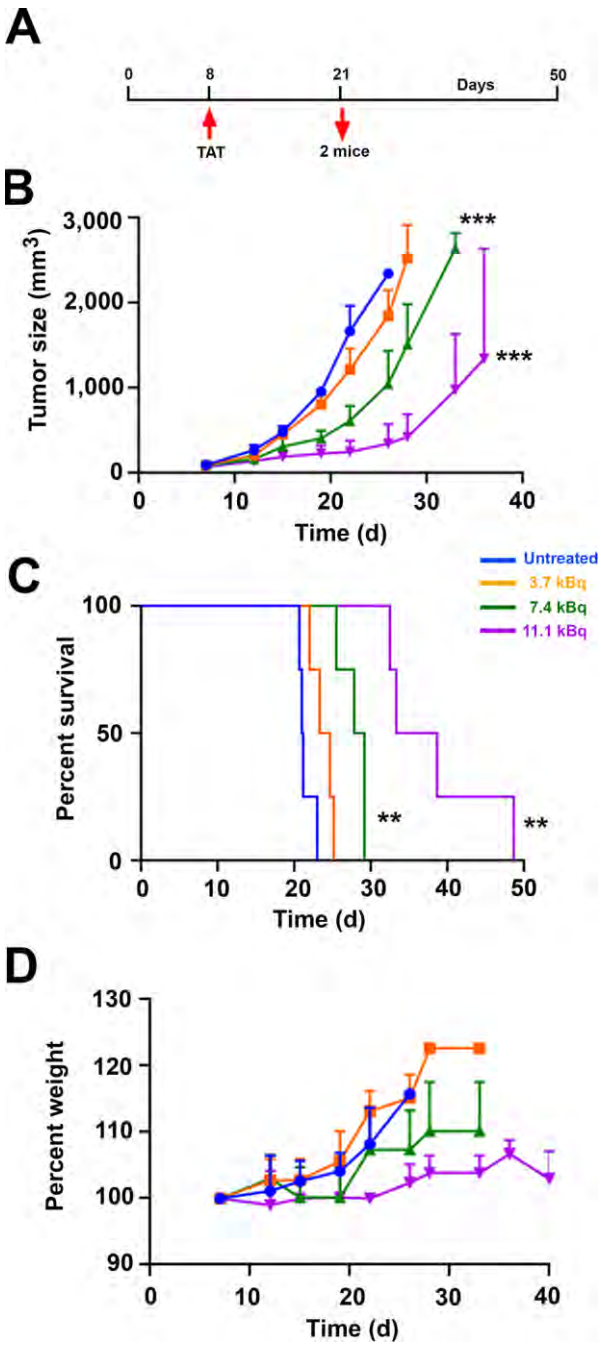

Figure 1. ^{225}Ac-DOTA-M5A TAT in an orthotopic breast cancer model. A. Treatment schema and color codes for TAT doses. Tumor growth curves (B), Kaplan-Meier survival plot (C) and weight loss (D). Group sizes were N=8 with two mice removed at days 21/22 for blood analysis. *** $p<0.001$; ** $p<0.01$; * $p<0.05$.

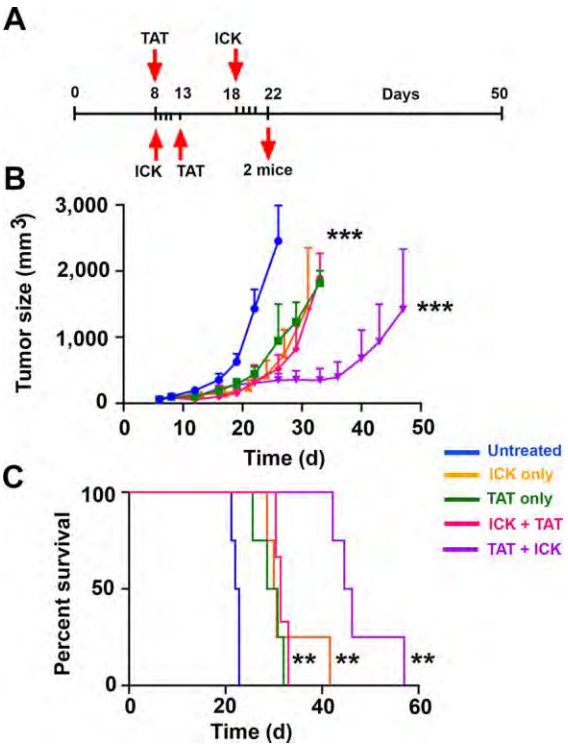

Figure 2. ICK first vs TAT first in sequential therapy in a breast cancer model. A. Treatment schema for ICK first followed by TAT (lower) or TAT first followed by ICK (upper). Group sizes were N=8 with two mice removed at days 21/22 for blood analysis. Tumor growth curves (B) and Kaplan-Meier survival plots (C) for ICK first vs TAT first sequential therapies. P values vs untreated controls, *** $p<0.001$; ** $p<0.01$; * $p<0.05$.

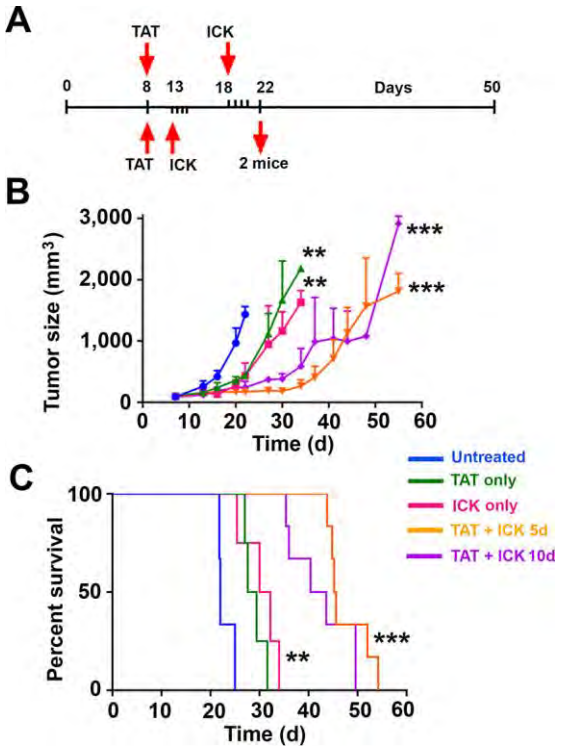

Figure 3. TAT followed by ICK, 5 or 10 days later in a breast cancer model. A. Treatment schema for TAT followed by ICK 5 days later (upper) or 10 days later (lower). Group sizes were N=8 with two mice removed at days 21/22 for blood analysis. Tumor growth curves (B) and Kaplan-Meier survival plots (C). P values vs untreated controls, *** $p<0.001$; ** $p<0.01$; * $p<0.05$.

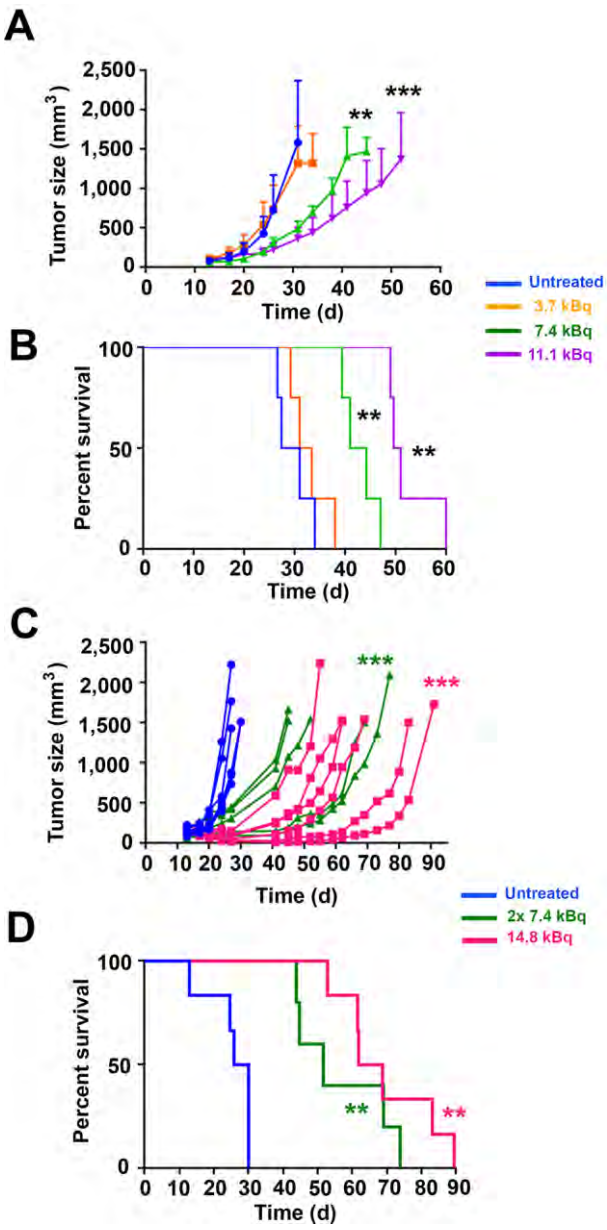

Figure 4. Dose response of TAT in a colon cancer model. A. Tumor growth curves (A) and Kaplan-Meier survival plot (B) for TAT dose response (N=6 per group, two removed at day 27). Tumor growth curves (C) and Kaplan-Meier survival plot (D) for 2x 7.4 kBq vs 14.8 kBq TAT, N=5-6. P values vs untreated controls, *** $p<0.001$; ** $p<0.01$; * $p<0.05$.

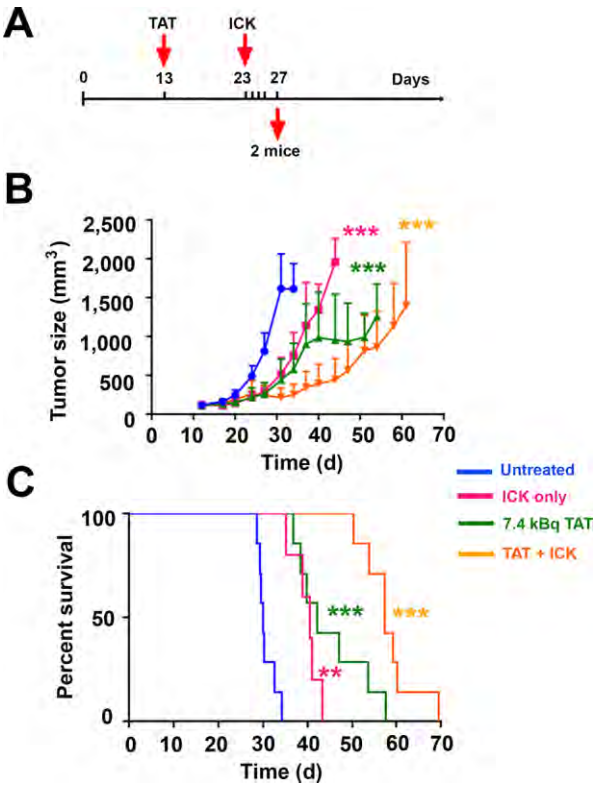

Figure 5. TAT first followed by ICK therapy in a colon cancer model. Treatment schema and TAT doses (A), tumor growth curves (B) and Kaplan-Meier survival plot (C), for TAT plus ICK sequential therapy, N=7 per group. P values vs untreated controls, *** $p<0.001$; ** $p<0.01$; * $p<0.05$

SUPPLEMENTAL METHODS

Immunohistochemistry, blood analysis and flow cytometry. (IHC) was carried out by the pathology core at City of Hope using the Ventana Discovery Ultra autostainer (Ventana Medical Systems, Roche Diagnostics, Indianapolis, USA) and the ChromoMap DAB detection system according to manufacturer's recommendations. Briefly, the tissue samples were collected and fixed in 4% paraformaldehyde for 3 days and then stored in 70% EtOH. The sampled were blocked in paraffin, sectioned at a thickness of 5 µm and put on positively charged glass slides. For hematoxylin & eosin (H&E) stains, the slides were deparaffinized, rehydrated and stained with Modified Mayer's Hematoxylin and Eosin Y Stain (America MasterTech Scientific) on a H&E Auto Stainer (Prisma Plus Auto Stainer, SAKURA) according to standard laboratory procedures. For the specific immunohistochemistry stains, the slides were loaded on the machine, deparaffinization, rehydration, endogenous peroxidase activity inhibition and antigen retrieval were first performed. Then, each primary antibody was incubated following by DISCOVERY anti-Rabbit HQ and DISCOVERY anti-HQ-HRP incubation. The stains were visualized with DISCOVERY ChromoMap DAB Kit, counterstained with hematoxylin (Ventana) and cover slipped. For humanized anti-human M5A antibody stains, Goat anti-human IgG antibody (H+L), biotinylated (Vector Laboratories) was used and followed by VECTOASTAIN ABC kits (HRP) and DAB. H&E or IHC stained slides were digitalized and documented by iScan HT (Roche) scanner.

Hematologic analysis was done using the VETSCAN HM5 Hematology Analyzer. Blood (50-100 µl) was collected and stored in EDTA tubes until analyzed, 1-2 hours post collection. For kidney and liver toxicity, about 400 µl blood was collected in lithium heparin tubes and spun down to separate RBCs and plasma. Plasma was collected and stored at -80C until analysis on the VETSCAN VS2 Chemistry Analyzer, using the Preventive Care Profile Plus rotors (Zoetis).

Tissues and blood were collected at time points indicated above, and leukocyte populations were analyzed by flow cytometry using gating strategy as published before. Blood samples were analyzed after red cells lysis using Red Blood Cell Lysis Buffer Hybri-Max (Sigma). Tumor draining lymph nodes and spleens were pushed through a 40µm cell strainer (Corning) and red cells were lysed. Tumors were dissociated by enzymatic digestion using gentleMacs Octo Dissociator and dissociation kit following the manufacture's protocol (Miltenyi Biotec). Cell suspensions were stained with different combinations of fluorochrome-coupled antibodies to CD3, CD4, CD8, CD19, CD11b, Ly6C, Ly6G, CD11c, F4/80, PD-1, CTLA-4, Tim-3 (BioLegend). For IFNγ production cells from all tissues were re-stimulated using Cell Activation Cocktail containing Brefeldin A(BioLegend) in 10% FBS IMDM media for 4 hours in 37ºC. Next, cells were stained for surface markers and viability marker (Zombie UV, BioLegend) and fixed and permeabilized using Foxp3 Transcription Factor Fixation/Permeabilization kit (ThermoFisher) following the manufacture's protocol. Finally, cells were stained for intracellular IFNγ (BioLegend) and analyzed by flow cytometry. For FoxP3 expression cells were stained for surface markers, fixed and permeabilized as described above and stained with anti-FoxP3 antibody (ThermoFisher).

SUPPLEMENTAL TABLES

Supplemental Table 1. Statistical analyses of tumor treatments[1]

Fig 1A	3.7kBq	7.4kBq	11.1kBq
Untr.	n.s.	***	***
3.7kBq		***	***
7.4kBq			***

Fig 1B	3.7kBq	7.4kBq	11.1kBq
Untr.	*	**	**
3.7kBq		**	**
7.4kBq			**

Fig 2A	TAT	ICK	ICK+TAT	TAT+ICK
Untr.	***	***	***	***
TAT		n.s.	n.s.	**
ICK+TAT		n.s.		***
TAT+ICK		*		

Fig 2B	TAT	ICK	ICK+TAT	TAT+ICK
Untr.	**	*	**	**
TAT		n.s.	n.s.	**
ICK+TAT		n.s.		**
TAT+ICK		*		

Fig 3A	TAT	ICK	TAT+ICK5d	TAT+ICK10d
Untr.	**	**	***	***
TAT		n.s.	**	**
ICK			***	**
TAT+ICK5d				n.s.

Fig 3B	TAT	ICK	TAT+ICK5d	TAT+ICK10d
Untr.	*	*	**	**
TAT		n.s.	**	**
ICK			**	**
TAT+ICK5d				n.s.

Fig 4A	3.7kBq	7.4kBq	11.1kBq
Untr.	n.s.	**	***
3.7kBq		***	***
7.4kBq			**

Fig 4B	3.7kBq	7.4kBq	11.1kBq
Untr.	n.s.	**	**
3.7kBq		**	**
7.4kBq			**

Fig 4C	14.8kBq	2x7.4kBq
Untr.	***	***
14.8kBq		n.s.

Fig 4D	14.8kBq	2x7.4kBq
Untr.	**	**
14.8kBq		n.s.

Fig 4E	ICK	TAT	TAT+ICK
Untr.	***	***	***
3.7kBq		n.s.	***
7.4kBq			**

Fig 4F	ICK	TAT	TAT+ICK
Untr.	**	***	***
3.7kBq		n.s.	***
7.4kBq			*

[1] Statistical analysis between all treatment groups using two-way ANOVA test. Statistical analysis results of survival curves using Log-rank (Mantel-Cox) test. n.s. – not significant; *** $p<0.001$; ** $p<0.01$; * $p<0.05$.

Supplemental Table 2: Kidney and liver toxicity associated with TAT and ICK therapies in a E0771/CEA breast cancer model[1].

	Kidney		Liver	
	BUN (mg/dL)	**CRE** (mg/dL)	**ALT** (U/L)	**AST** (U/L)
Murine Normal	22±5	0.5±0.17	40±21	141±67
Saline	23±4	0.30±0.13	36±6	266±85
3.7kBq ^{225}Ac-M5A	22±3	0.45±0.13	39±6	352±138
7.4kBq ^{225}Ac-M5A	24.1±4	0.30±0.08	41±2	354±88
11.1kBq ^{225}Ac-M5A	25±5	0.50±0.15	41±3	369±73
ICK	26±2	0.3±0.17	34±5	168±24
ICK+7.4kBq TAT	21±1	0.2±0.07	37±3	292±62
7.4kBq TAT+ICK	25±3	0.2±0.14	46±10	303±94

[1] Liver Toxicity: alanine aminotransferase (ALT)/ aspartate aminotransferase (AST); Kidney Toxicity: Blood Urea Nitrogen (BUN)/ creatinine (CRE). Plasma analyzed at end point of each mouse. Average of N=4.

Supplemental Table 3: Median Survival of E0771/CEA Experiments[1].

	Saline	**3.7kBq TAT**	**7.4kBq TAT***	**11.1kBq TAT**	**ICK**	**ICK+ 7.4kBq TAT**	**7.4kBq TAT+ ICK(18d)**	**7.4kBq TAT+ ICK(13d)**
Median Survival	21.8	24.0	28.9	36.0	31.2	30.2	43.7	45.4

[1] Average of all groups.

Supplemental Table 4: Median survival of TAT and ICK therapies in a Colon Cancer MC38/CEA Model[1].

	Saline	3.7kBq TAT	7.4kBq TAT	11.1kBq TAT	ICK	7.4kBq TAT+ ICK	7.4kBq TAT x 2	14.8kBq TAT
Median Survival	29.1	32.2	42.3	50.2	40.6	57.3	51.5	65.3

[1]Average of all groups.

Supplemental Table 5: Kidney and Liver Toxicity associated with TAT and ICK therapies in a Colon Cancer MC38/CEA Model[1].

	BUN (mg/dL)	CRE (mg/dL)	ALT (U/L)	AST (U/L)
Murine Normal	22±5	0.5±0.17	40±21	141±67
Saline	30±2	0.22±0.05	24±6	198±81
7.4kBq TAT+ICK	26±3	0.22±0.04	96±20	264±67
7.4kBq ^{225}Ac-M5A x2	27±3	0.25±0.06	35±11	185±9
14.8kBq ^{225}Ac-M5A	24±2	0.3±0.14	36±13	154±32

[1] Liver Toxicity: alanine aminotransferase (ALT)/ aspartate aminotransferase (AST); Kidney Toxicity: Blood Urea Nitrogen (BUN)/ creatinine (CRE). Plasma analyzed at end point of each mouse. N=4-5

SUPPLEMENTAL FIGURES

Supplemental Figure 1. Immunophenotyping of ^{225}Ac-DOTA-M5A TAT in an orthotopic breast cancer model. Analysis of CD4, CD8, B and CD11b cells in the blood (**A**) and tumor (**B**). Tumor infiltrating neutrophils to CD11b cell ratio (**C**). P values vs untreated controls, *** p<0.001; ** p<0.01; * p<0.05.

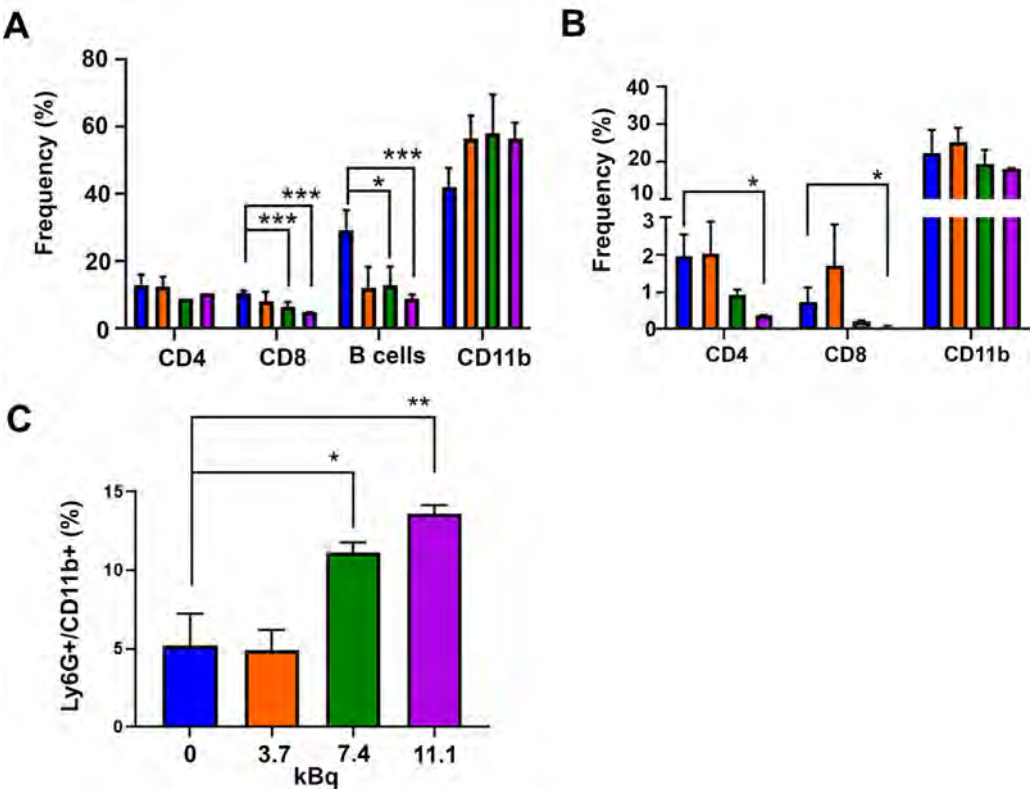

Supplemental Figure 2. Whole body toxicity and hematologic analysis of combination therapy, varying order of therapy, in E0771/CEA mice. (**A**) Whole body weights, a measure of toxicity. (**B-F**) Early time point was collected 21-22 days post E0771/CEA injection, N=2. End time point was collected as each mouse reached the 1500mm^3 end point, N=4. (**B**) White Blood Cell counts. (**C**) Leukocytes counts. (**D**) Leukocyte percents. (**E**) Red Blood Cell counts. (**F**) Platelets counts.

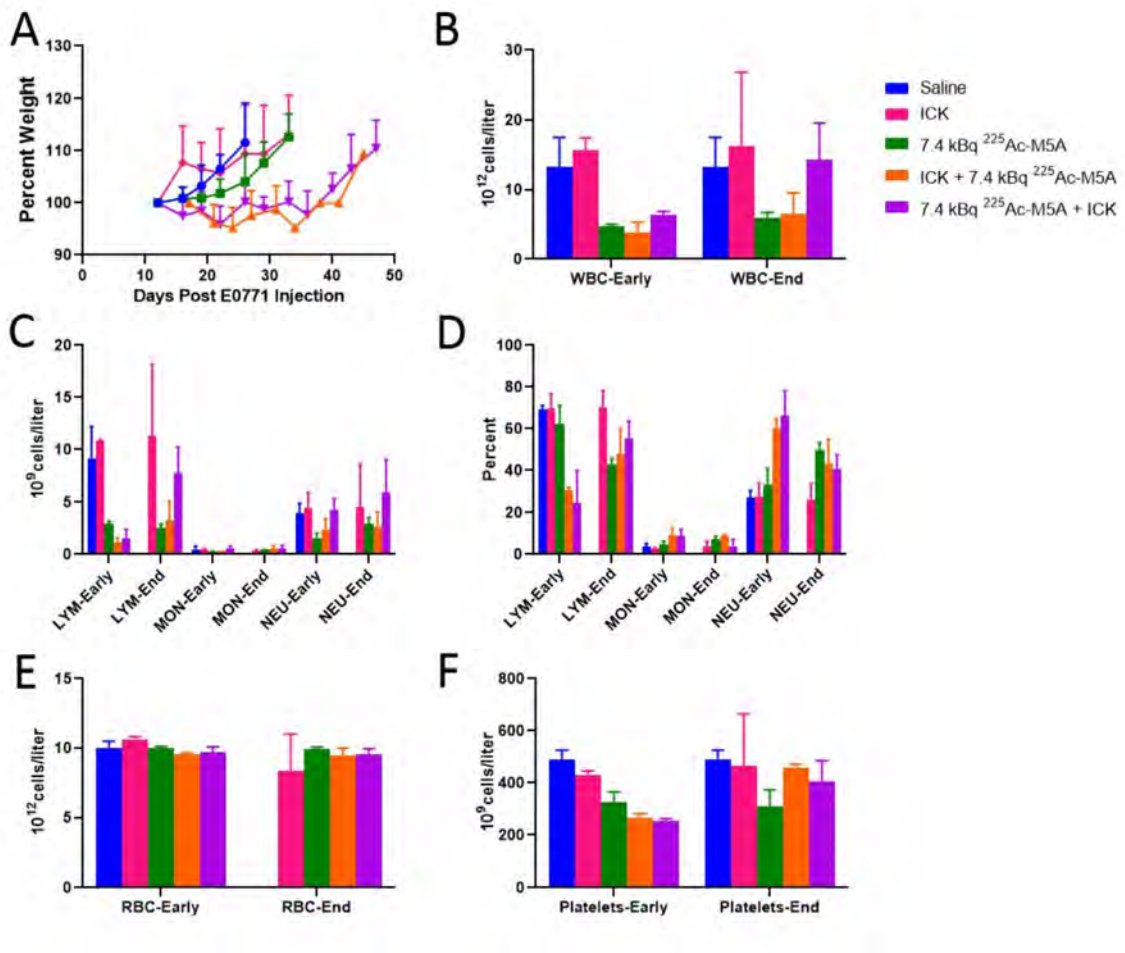

Supplemental Figure 3. Immunophenotyping of ICK first vs TAT first in sequential therapy in a breast cancer model. Analysis of CD4 (white) and CD11b (grey) cells in tumors (**A).** Percent of IFNγ^{+} /CD8^{+} T-cells in spleen (black), TDLNs (white) and tumor (grey) (**B**). Percent of IFNγ^{+}/PD-1^{-} (black), IFNγ^{+}/PD-1^{+} (white) and IFNγ^{-}/PD-1^{+} (grey) populations of tumor infiltrating CD8^{+} T-cells (**C**). Ratio of IFNγ^{+}/CD8^{+} T-cells to Foxp3^{+}/CD4^{+} regulatory T-cells in tumors (**D**). P values vs untreated controls, *** p<0.001; ** p<0.01; * p<0.05.

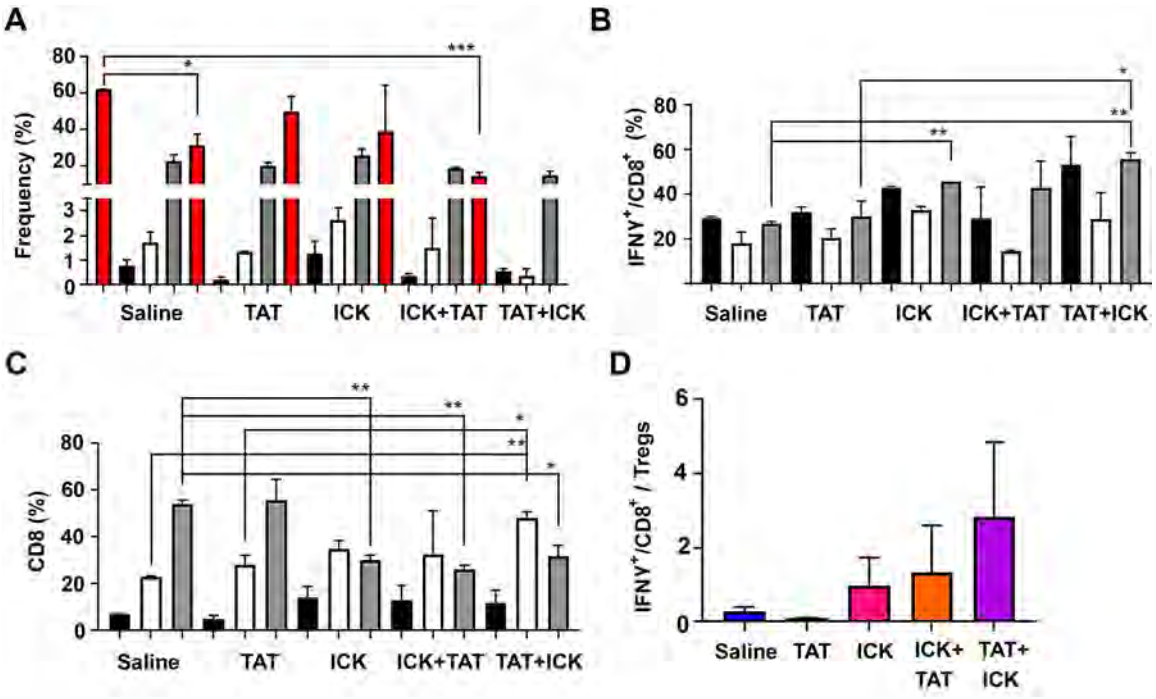

Supplemental Figure 4. Immunophenotyping of TAT followed by ICK, 5 or 10 days later in a breast cancer model. Analysis of cell viability (red), and frequency of CD8 (black), CD4 (white) and CD11b (grey) cells in tumors (**A**). Percent of $FoxP3^+$ /$CD4^+$ T-cells for different treatment groups (**B**). Percent of $IFN\gamma^+$ $CD8^+$ as % of CD8 cells (black) or % of viable cells (red) (**C**). Ratio of $IFN\gamma^+/CD8^+$ T-cells to $Foxp3^+/CD4^+$ regulatory T-cells in tumors (**D**). P values vs untreated controls, *** p<0.001; ** p<0.01; * p<0.05.

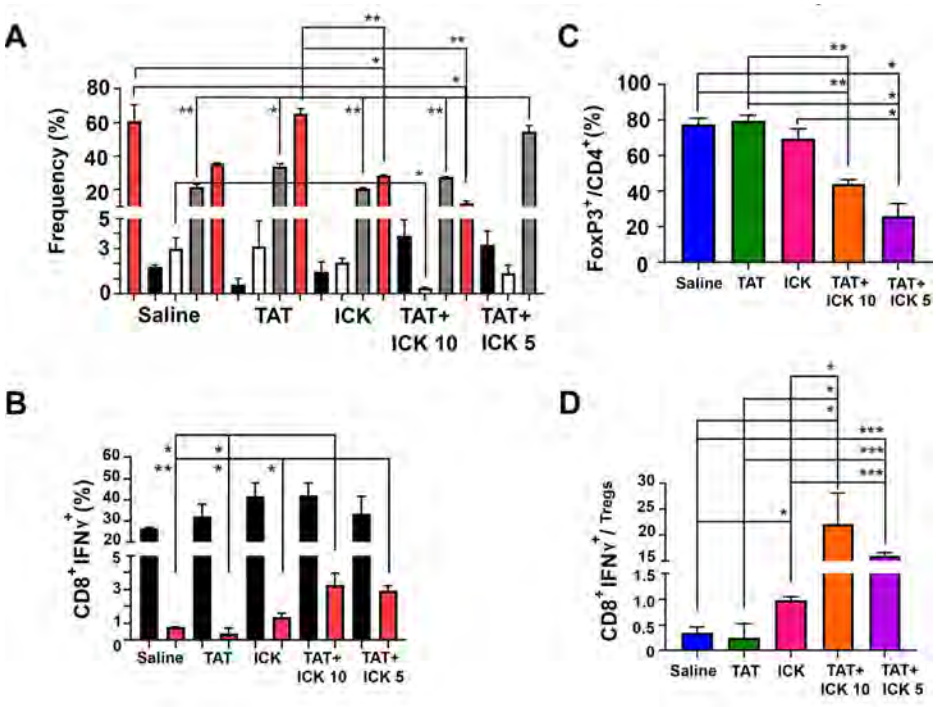

Supplemental Figure 5. Whole body toxicity and hematologic analysis of combination therapy, with ICK 5 or 10 days post TAT, in E0771/CEA mice. (**A**) Whole body weights, a measure of toxicity. (**B-F**) Early time point was collected 22 days post E0771/CEA injection, N=2. End time point was collected as each mouse reached the 1500mm^3 end point, N=4. (**B**) White Blood Cell counts. (**C**) Leukocytes counts. (**D**) Leukocyte percents. (**E**) Red Blood Cell counts. (**F**) Platelets counts.

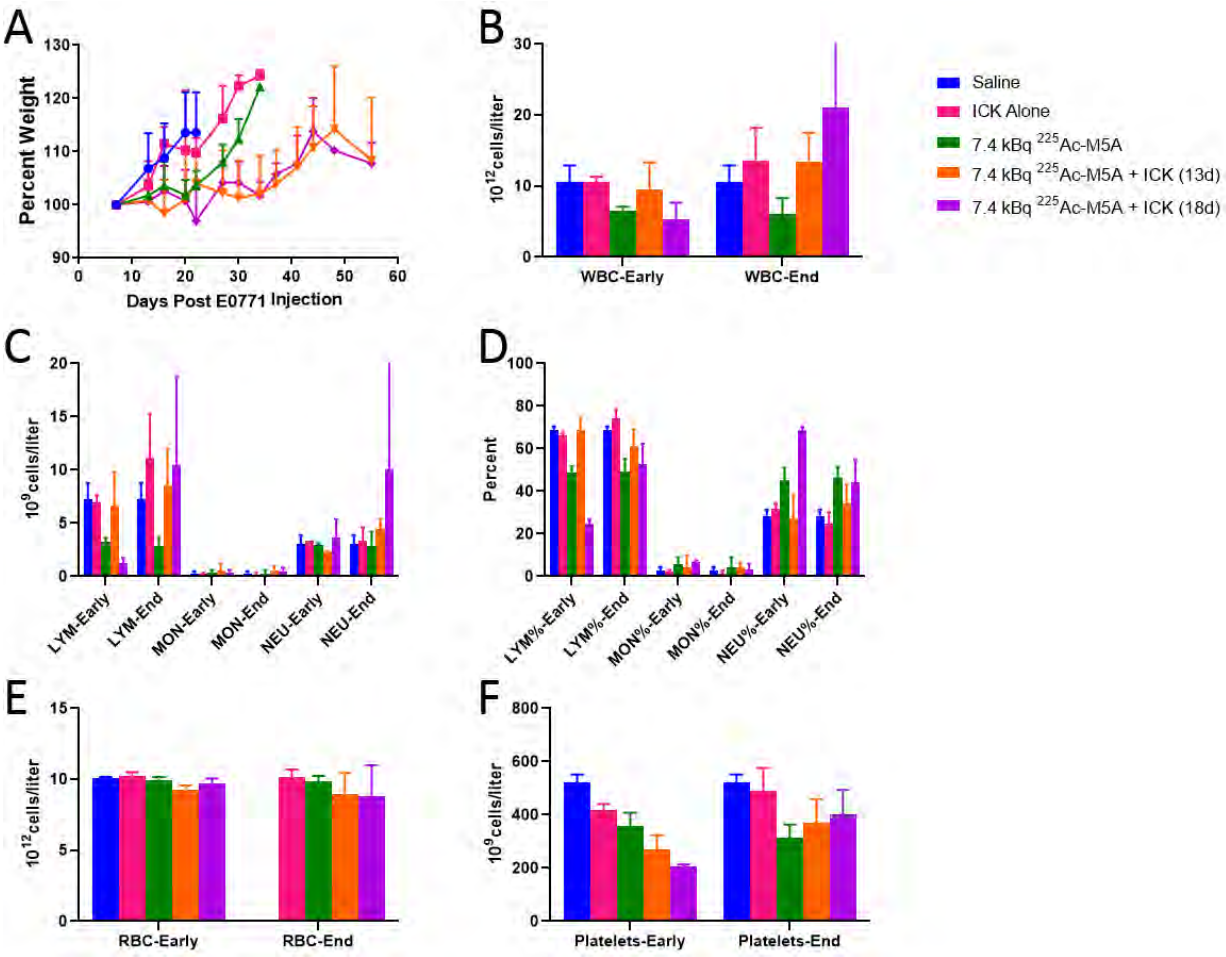

Supplemental Figure 6. Whole body toxicity and hematologic analysis of dose escalation study in MC38/CEA engrafted mice. (**A**) Whole body weights, a measure of toxicity. (**B-F**) Early time point was collected 22 days post E0771/CEA injection, N=2. End time point was collected as each mouse reached the 1500mm^3 end point, N=4. (**B**) White Blood Cell counts. (**C**) Leukocytes counts. (**D**) Leukocyte percents. (**E**) Red Blood Cell counts. (**F**) Platelets counts.

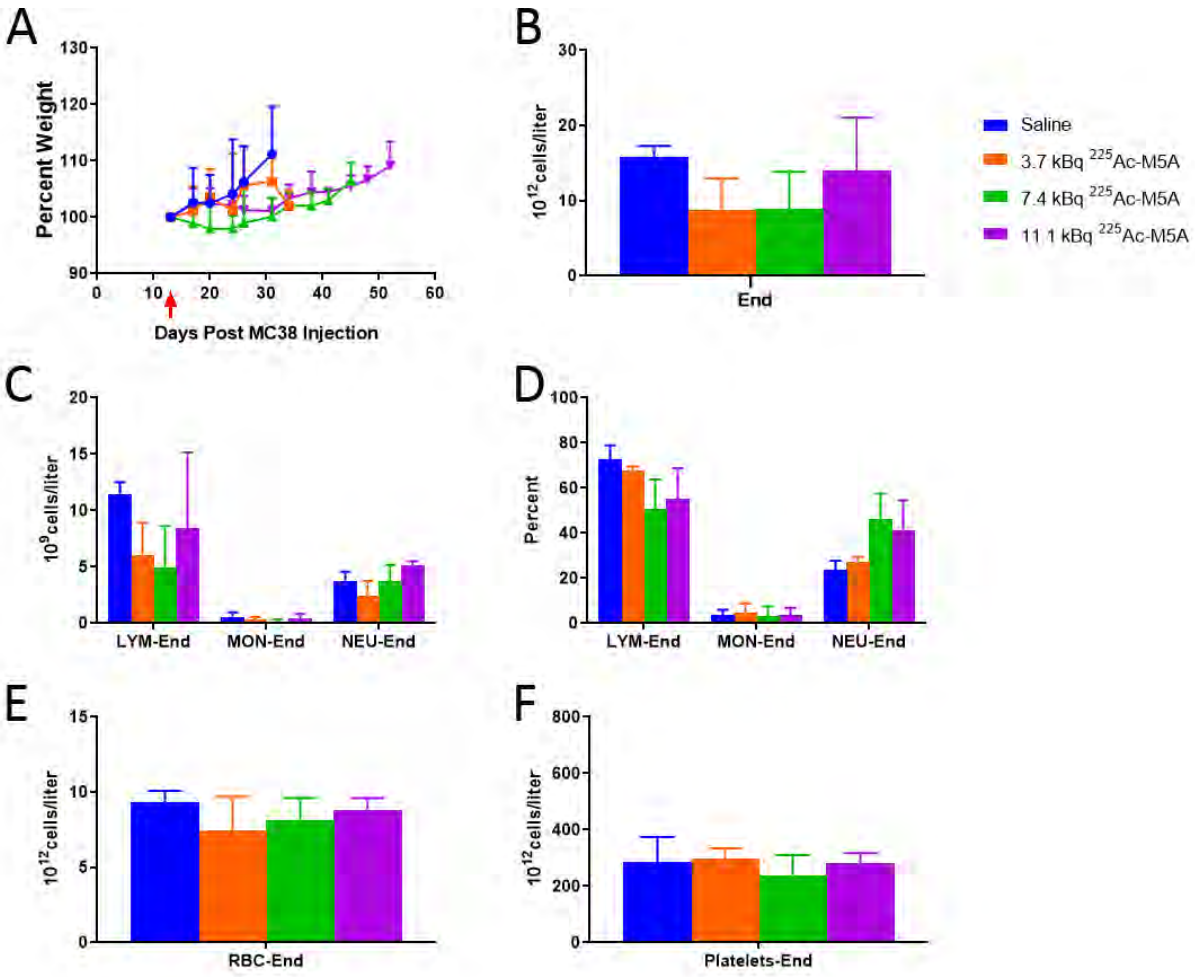

Supplemental Figure 7. Whole body toxicity and hematologic analysis of combination therapy in MC38/CEA engrafted mice. (**A**) Whole body weights, a measure of toxicity. (**B-F**) Early time point was collected 22 days post E0771/CEA injection, N=2-3. End time point was collected as each mouse reached the 1500mm^3 end point, N=2-3. (**B**) White Blood Cell counts. (**C**) Leukocytes counts. (**D**) Leukocyte percents. (**E**) Red Blood Cell counts. (**F**) Platelets counts.

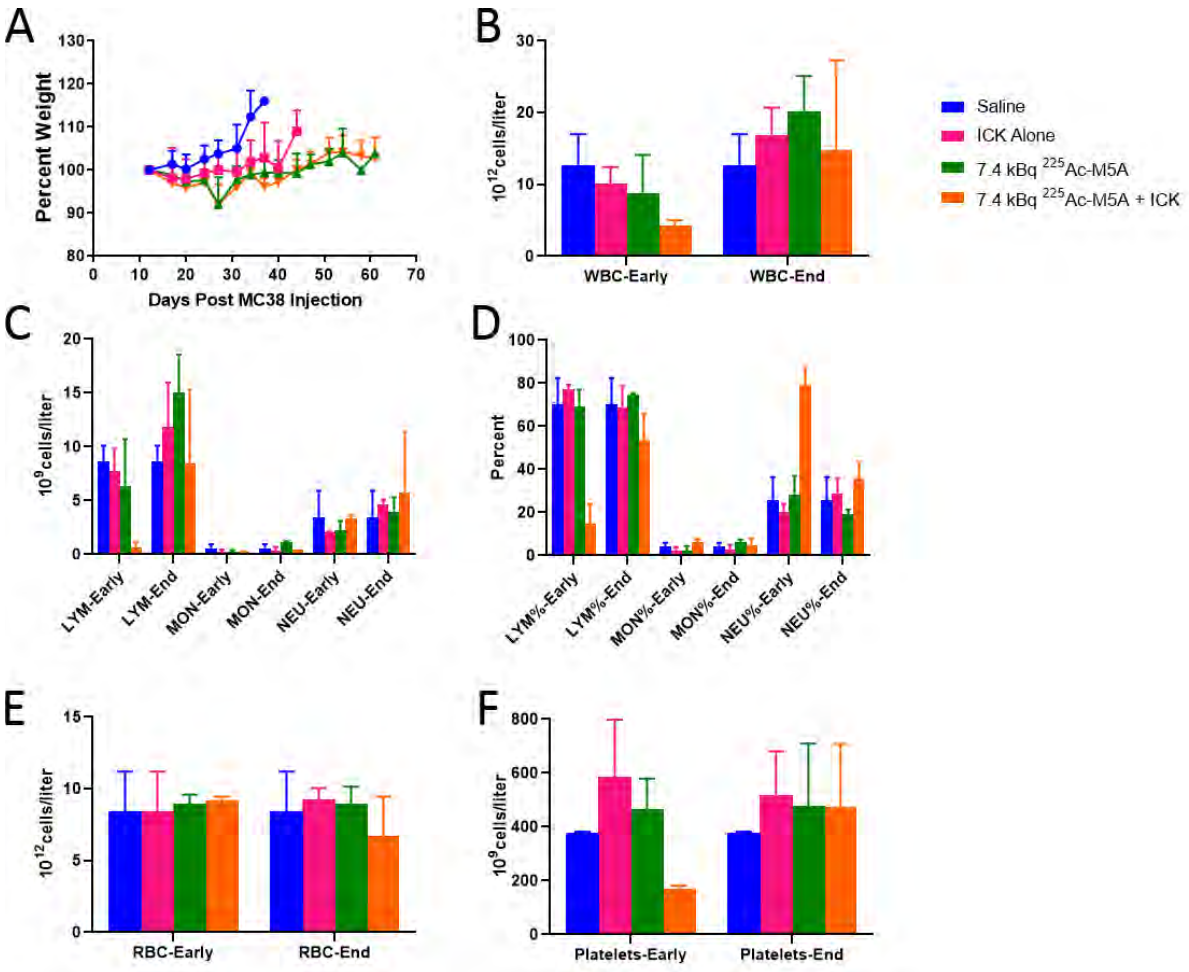

Supplemental Figure 8. Phenotyping of TAT first followed by ICK therapy in a colon cancer model. Analysis of Live cells (red), CD4 (black), CD8 (white) and CD11b (grey) cells in tumors analyzed by flow cytometry at day 27 (**A**). IFNγ$^+$ CD4$^+$ (black) and CD8$^+$ (white) cells in tumors analyzed by flow cytometry at day 27 (**B**). CD4 (black) and CD8 (white) cells in tumors analyzed at days 1, 5 and 8 after last dose of ICK in TAT+ICK group (**C**). Tumor infiltrating IFNγ$^+$ CD8$^+$ cells at days 1, 5 and 8 after last dose of ICK in TAT+ICK group (**D**). Ratio of IFNγ$^+$ CD8$^+$ T-cells to regulatory T-cells in tumors at days 1, 5 and 8 after last dose of ICK in TAT+ICK group (**E**). P values vs untreated controls, *** p<0.001; ** p<0.01; * p<0.05

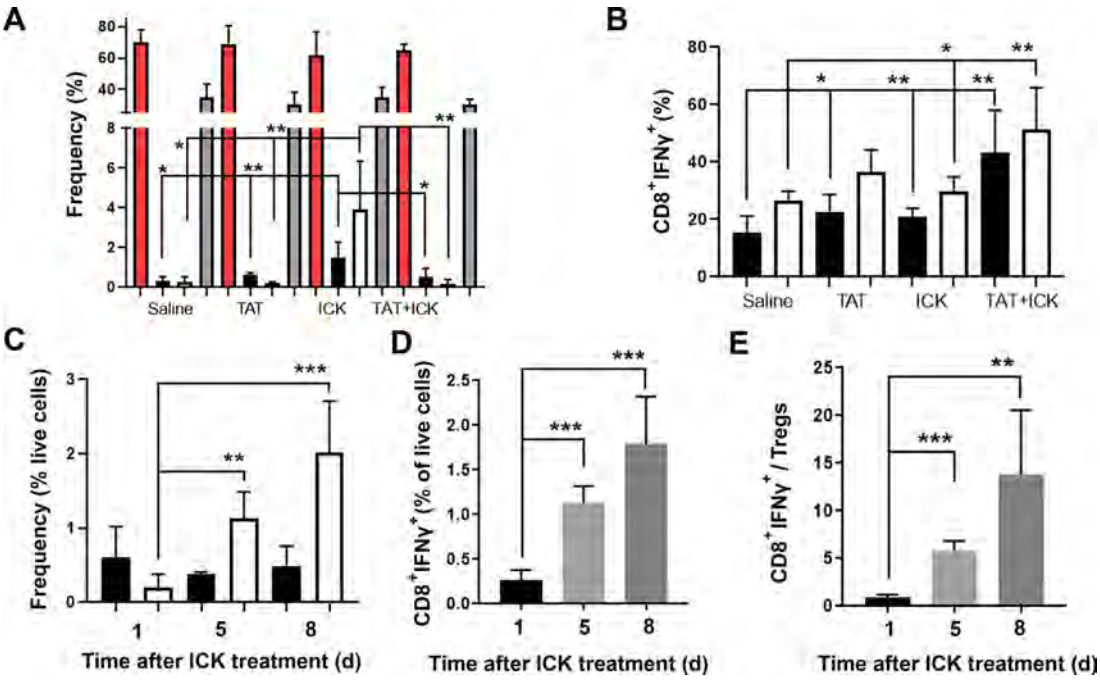

Supplemental Figure 9. CD31 staining of E0771/CEA breast and MC38/CEA colon cancer tumors. A-D, CD31 staining for E0771/CEA breast cancer tumors in untreated controls (**A**), TAT only (**B**), ICK only (**C**), and combination therapy (**D**). **E- F**, CD31 staining for MC38/CEA colon tumors in untreated controls (**E**), TAT only (**F**), ICK only (**G**), and combination therapy (**H**). 10x magnification.

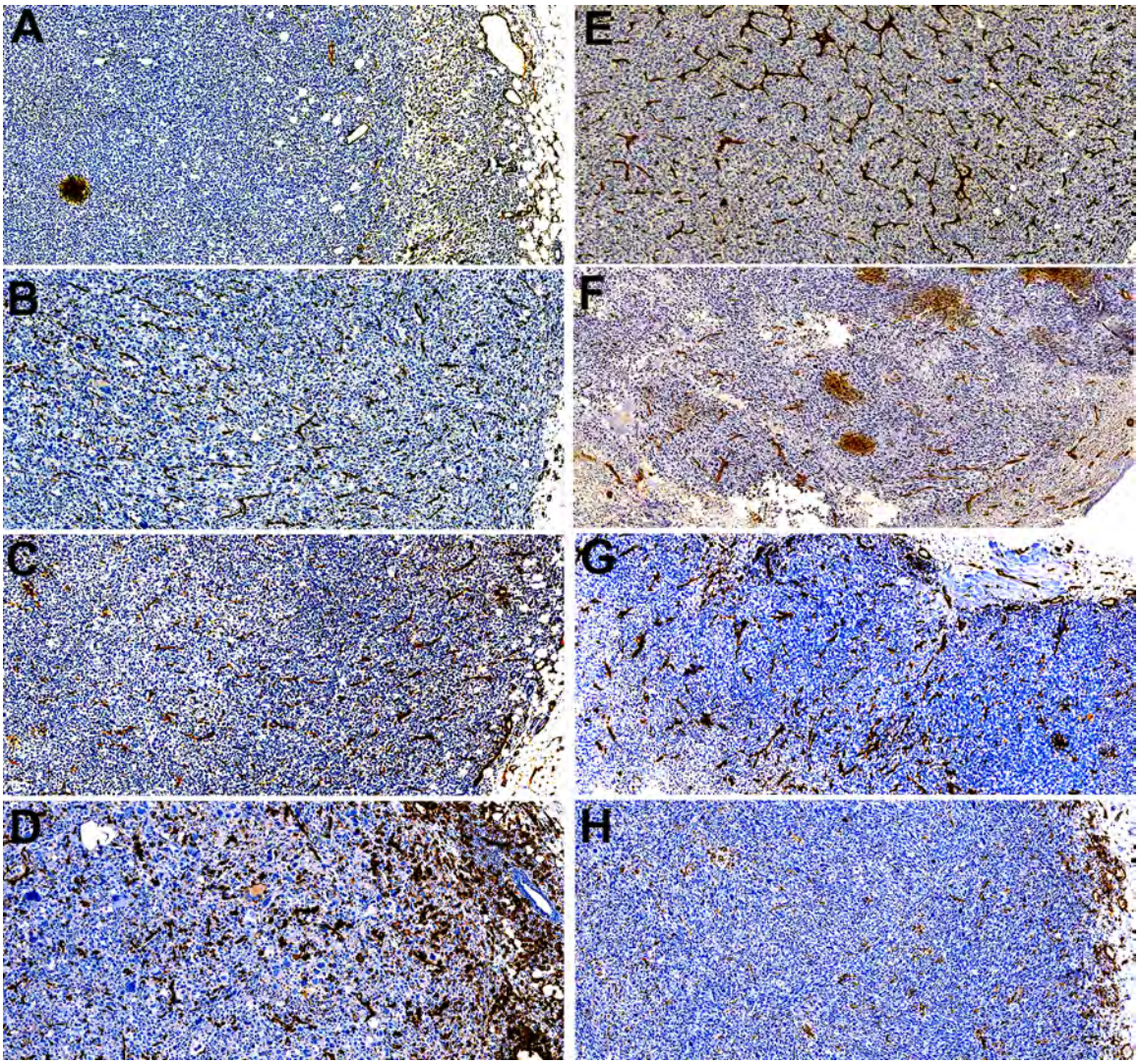

Supplemental Figure 10. CD8 and CEA staining of E0771/CEA breast cancer tumors. A-D, CD8 staining in untreated controls (**A**), TAT only (**B**), ICK only (**C**), and combination therapy (**D**). **E- F**, CEA staining in untreated controls (**E**), TAT only (**F**), ICK only (**G**), and combination therapy (**H**). 10x magnification.

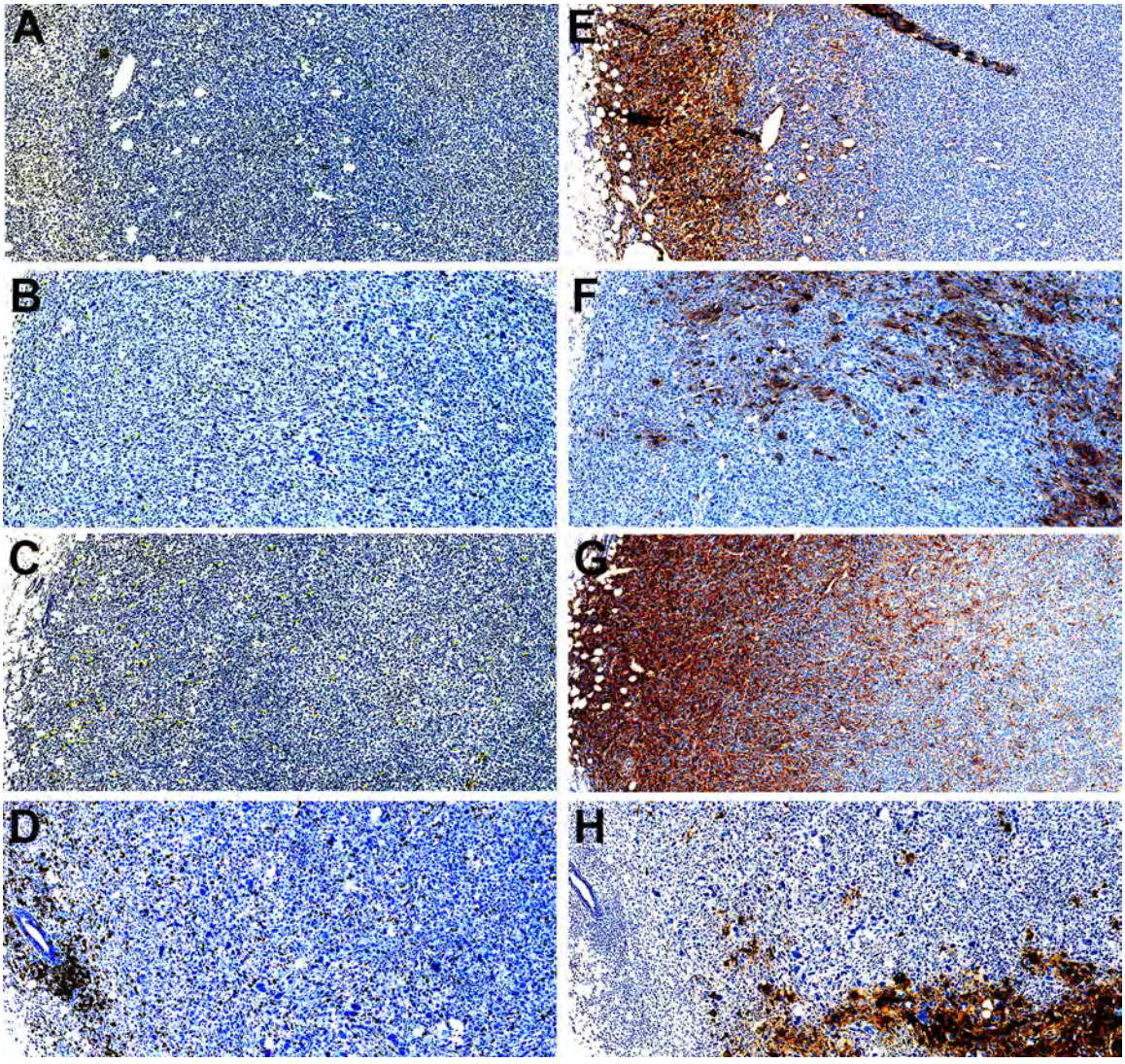

Supplemental Figure 11. F4-80 staining of E0771/CEA breast cancer tumors. F4-80 staining in untreated controls (**A**), TAT only (**B**), ICK only (**C**), and combination therapy (**D**). 10x magnification.

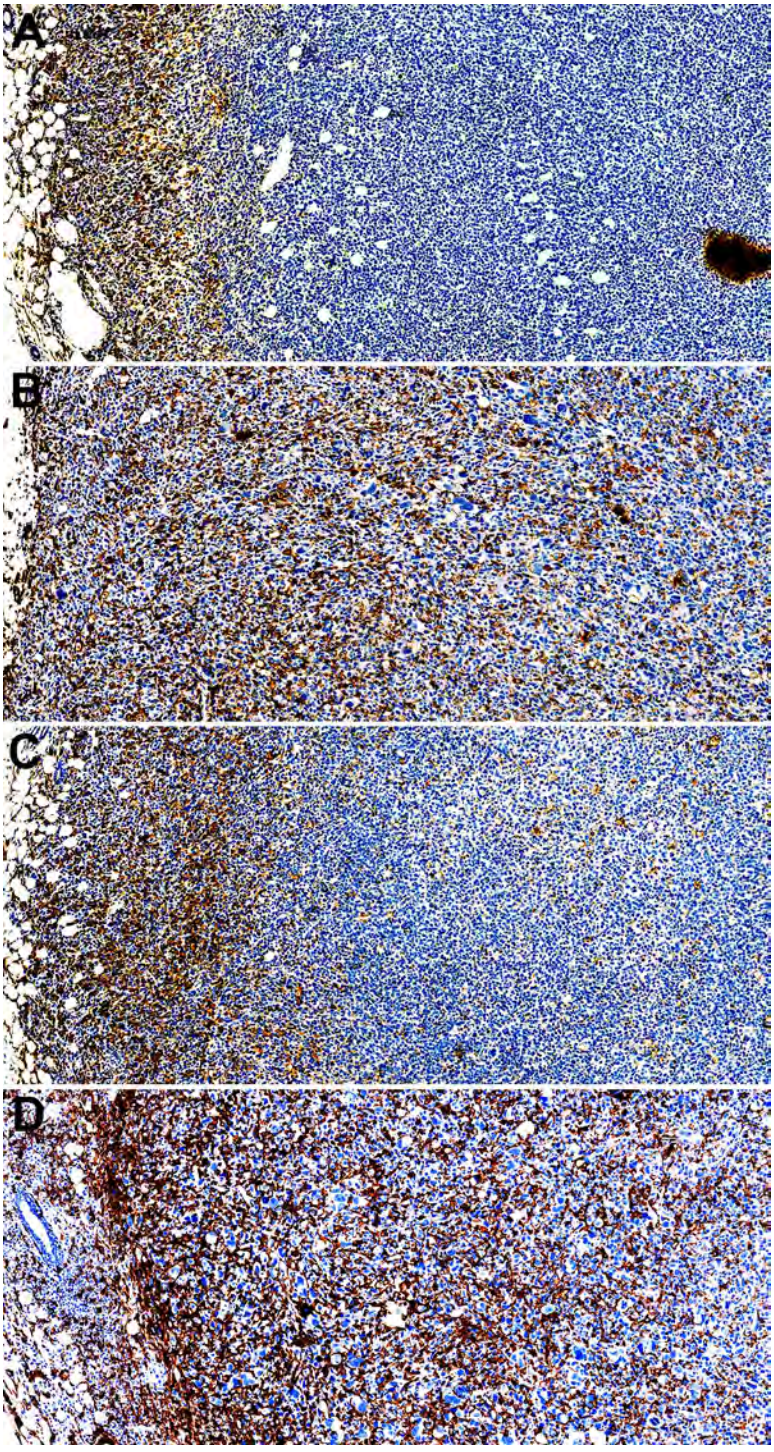

Supplemental Figure 12. CD8 and CEA staining of MC38/CEA colon cancer tumors. A-D, CD8 staining in untreated controls (**A**), TAT only (**B**), ICK only (**C**), and combination therapy (**D**). **E- F**, CEA staining in untreated controls (**E**), TAT only (**F**), ICK only (**G**), and combination therapy (**H**). 10x magnification.

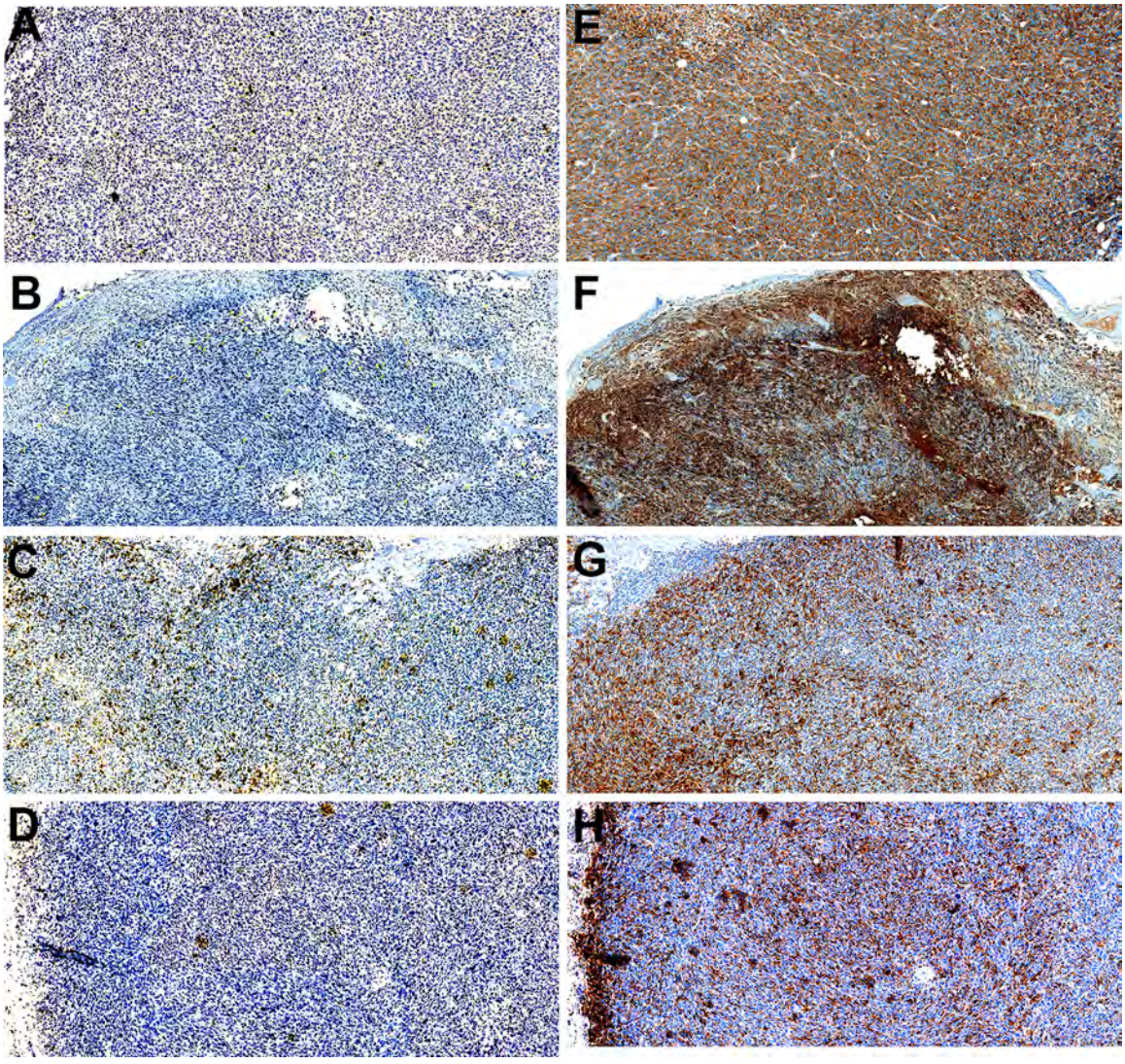

Supplemental Figure 13. F4-80 staining of MC38/CEA colon cancer tumors. F4-80 staining in untreated controls (**A**), TAT only (**B**), ICK only (**C**), and combination therapy (**D**). 10x magnification.